Lysine 190 Is the Catalytic Base in MenF, the Menaquinone-Specific Isochorismate Synthase from *Escherichia coli*: Implications for an Enzyme Family†

Subramaniapillai Kolappan,[‡,§,||] Jacque Zwahlen,[§,⊥] Rong Zhou,[⊥] James J. Truglio,[‡] Peter J. Tonge,*[,⊥] and Caroline Kisker*[,‡,#]

Department of Pharmacological Sciences and Center for Structural Biology, Stony Brook University, Stony Brook, New York 11794-5115, Department of Chemistry, Stony Brook University, Stony Brook, New York 11794-3400, and Rudolf Virchow Center for Experimental Biomedicine, Institute for Structural Biology, University of Würzburg, Versbacher Str. 9, 97078 Würzburg, Germany

Received May 1, 2006; Revised Manuscript Received August 20, 2006

ABSTRACT: Menaquinone biosynthesis is initiated by the conversion of chorismate to isochorismate, a reaction that is catalyzed by the menaquinone-specific isochorismate synthase, MenF. The catalytic mechanism of MenF has been probed using a combination of structural and biochemical studies, including the 2.5 Å structure of the enzyme, and Lys190 has been identified as the base that activates water for nucleophilic attack at the chorismate C2 carbon. MenF is a member of a larger family of Mg^{2+} dependent chorismate binding enzymes catalyzing distinct chorismate transformations. The studies reported here extend the mechanism recently proposed for this enzyme family by He et al.: He, Z., Stigers Lavoie, K. D., Bartlett, P. A., and Toney, M. D. (2004) *J. Am. Chem. Soc. 126,* 2378−85.

Menaquinone (MK) is a chorismate-derived metabolite essential for electron transport and ATP synthesis in both aerobic and anaerobic bacteria (*1*). In humans, who are unable to synthesize MK, it is essential for blood clotting and is obtained from both intestinal flora and dietary sources (*2*). MK is synthesized by the coordinated activity of up to eight menaquinone-specific genes (*menA*−*menH*) lacking human homologues and each representing a potentially novel drug target (*3*). Inhibitors of menaquinone biosynthesis may be particularly effective against pathogens such as *Mycobacterium tuberculosis* (Mtb), which rely solely on menaquinone for oxidative phosphorylation (*4*). Although an obligate aerobe, Mtb is able to maintain infection under reduced oxygen conditions for more than a decade in a state of nonreplicating persistence (*5*). Recent studies have shown that inhibitors of the Mtb type II NADH:menaquinone oxidoreductase are bactericidal (*6*).

Like numerous other metabolites, including siderophores and aromatic amino acids, MK is derived from chorismate (*1*). The initial transformation is performed by a menaquinone-specific isochorismate synthase (ICS), normally annotated as *menF*. Interestingly, in the Mtb H37Rv genome, no annotated *menF* gene has been identified. A putative ICS, annotated as *entC*, is located more than one million base pairs from a cluster of other *men* genes (*7*). As a prelude to characterizing the Mtb ICS, we focus here on the *Escherichia coli* MenF,[1] which is a component of the menaquinone operon in this organism. MenF is a member of a larger family of chorismate binding enzymes that has descended from a common ancestor. As this family catalyzes the initial reactions in menaquinone, siderophore, and tryptophan biosynthesis, it will be hereafter referred to as the MST enzyme family. Common transformations of chorismate are shown in Figure 1 and include those catalyzed by the isochorismate synthase (ICS) enzymes MenF, EntC, and PchA, the salicylate synthases (SS) MbtI and Irp9, the anthranilate synthase (AS), and the aminodeoxychorismate synthases (PabB). Additional enzymatic reactions of chorismate are performed by the evolutionally distinct chorismate mutases (AroH and AroQ) (*8*) and chorismate lyases (UbiC) (*9*).

High affinity MST inhibitors, designed to mimic the isochorismate synthase transition state, have been reported (*10*). All known MST enzymes are Mg^{2+} dependent, and

† This work was supported by National Institutes of Health Research Grant AI58785 (to P.J.T.). J.Z. was partially supported by a GAANN (Graduate Assistance In Areas Of National Need) Fellowship.

* To whom correspondence should be addressed. P.J.T.: Department of Chemistry, Stony Brook University, Stony Brook, NY 11794-3400; tel, (631) 632 7907; fax, (631) 632 7934; e-mail, peter.tonge@sunysb.edu. C.K.: Rudolf Virchow Center for Experimental Biomedicine, Institute for Structural Biology, University of Würzburg, Versbacher Str. 9, 97078 Würzburg, Germany; tel, +0931 201 48300; fax, +0931 201 48309; e-mail, caroline.kisker@virchow.uni-wuerzburg.de.

‡ Department of Pharmacological Sciences and Center for Structural Biology.

§ These authors contributed equally to the work.

|| Present address: Simon Fraser University, Department of Molecular Biology and Biochemistry, Burnaby, BC Canada, V5A 1S6.

⊥ Department of Chemistry.

Rudolf Virchow Center for Experimental Biomedicine.

[1] Abbreviations: MenF, the menaquinone-specific isochorismate synthase from *E. coli*; PabB, aminodeoxychorismate synthase; AS, anthranilate synthase; AS-sm anthranilate synthase from *Serratia marcescens*; AS-ss, anthranilate synthase from *Sulfolobus solfataricus*; AS-st, anthranilate synthase from *Salmonella typhimurium*; TrpG, the glutamine amido transferase subunit of anthranilate synthase; MbtI, the salicylate synthase from *Mycobacterium tuberculosis*; Irp9, the salicylate synthase from *Yersinia enterocolitica*; MST, the related enzymes catalyzing the initial transformations in menaquinone, siderophore, and tryptophan biosynthesis.

10.1021/bi0608515 CCC: $37.00
Published on Web 01/06/2007

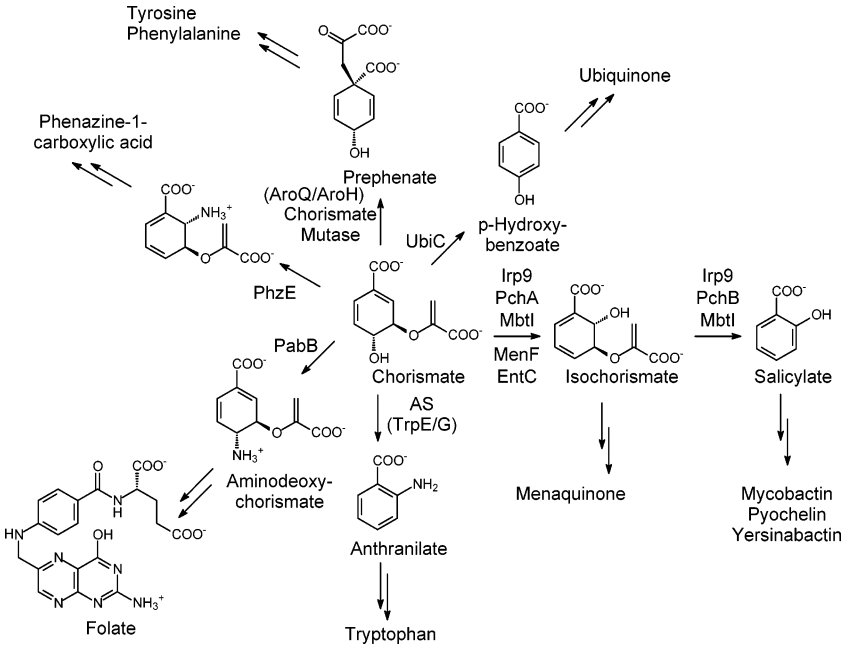

FIGURE 1: Enzymatic transformations of chorismate and their incorporation into aromatic products. With the exception of chorismate mutase (AroQ and AroH) and chorismate lyase (UbiC) all shown chorismate transformations are catalyzed by members of a related family of chorismate binding enzymes. Reactions shown include isochorismate synthase (MenF, PchA, and EntC), salicylate synthase (MbtI and Irp9), anthranilate synthase (AS), aminodeoxychorismate synthase (PabB), and aminodeoxyisochorismate synthase (PhzE).

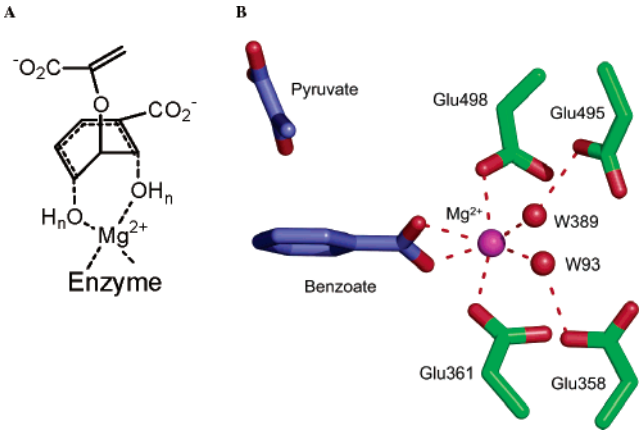

FIGURE 2: Proposed conformations of bound Mg^{2+} in the MST family. (A) Transition state for isochorismate synthase and related enzymes proposed by Walsh et al. (*11*) where Mg^{2+} was proposed to simultaneously coordinate the incoming nucleophile and the departing C4 hydroxyl. (B) Interactions involving Mg^{2+} in the crystal structure of anthranilate synthase from *Serratia marcescens* (PDB ID 1I7Q). The cluster of residues coordinating Mg^{2+} is highly conserved and includes the C1 carboxylate of the substrate/product. The figure was created using pymol (*40*).

studies utilizing the series of inhibitors synthesized by Kozlowski et al. support the Mg^{2+} bound transition state originally proposed by Walsh et al. (*11*) (Figure 2A). However, the crystal structure of AS from *Serratia marcescens* (AS-sm) in complex with Mg^{2+}, pyruvate, and benzoate (*12*) demonstrates that the Mg^{2+} is coordinated via conserved glutamate residues and the benzoate C1 carboxyl group in a conformation distinct from that originally proposed (Figure 2B). Similar Mg^{2+}−protein ligand interactions are also observed in the recently reported structure of salicylate bound to Irp9, the salicylate synthase from *Yersinia enterocolitica* (*13*).

Using a PabB model, He et al. have proposed a general mechanism for catalysis in the MST enzyme family (*14*).

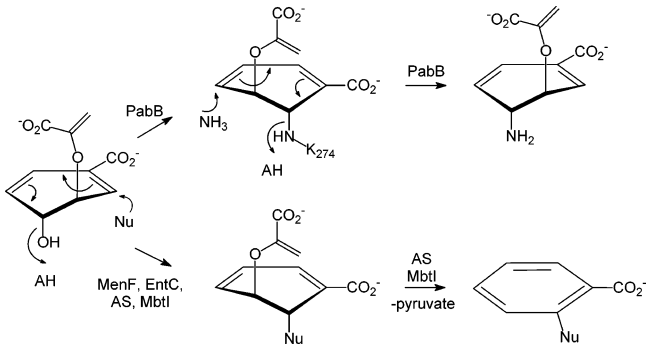

FIGURE 3: S_N2'' reaction mechanism adapted from He et al. (*14*). An incoming nucleophile attacks the C2 carbon of chorismate resulting in an S_N2'' reaction. In *E. coli* PabB this nucleophile is the ϵ-amino of Lys274. In all other members of the enzyme family it is an exogenous ammonia or solvent hydroxide molecule.

Based on a combination of biochemical studies and molecular modeling they proposed an S_N2'' mechanism in which catalysis is initiated by the attack of either an exogenous or main chain nucleophile at the C2 carbon of chorismate (Figure 3). In MenF and AS the exogenous nucleophiles are water and ammonia, respectively, while in *E. coli* PabB the amino side chain of Lys274 is the nucleophile. The PabB reaction thus proceeds via formation of a covalent enzyme−substrate intermediate (*15*), which yields the aminodeoxychorismate product following a second S_N2'' reaction initiated by attack of ammonia at C4 (*14*, *16*).

In the present work, we have determined the three-dimensional structure of *E. coli* MenF in the apo form. Comparison of this structure with those of other MST family members, coupled with a kinetic analysis of wild-type (WT) and mutant enzymes, reveals that Lys190 in MenF is in a position to activate a water molecule for attack at the chorismate C2 carbon, without direct involvement of the Mg^{2+} ion. The proposed mechanism reconciles previous data on the structure and inhibition of isochorismate synthase

(*10*−*12*) and adds further details to He et al.'s unified mechanism for catalysis in this enzyme family.

MATERIALS AND METHODS

Protein Expression and Purification. Chorismate was purified from the *E. coli* strain KA12 as previously described (*17*). *E. coli menF* and *entB* were cloned from *E. coli* BL21 whole cell lysate. All primers were synthesized by Integrated DNA Technologies (Coralville, IA). A 1 mL sample of a log phase culture was centrifuged and resuspended in 100 μL of H_2O, and 0.2−1.0 μL was then used as template in a standard 50 μL PCR reaction using Stratagene (La Jolla, CA) Pfu polymerase. An initial 6 min 95 °C denaturation step was used to disrupt the cells. The *entB* gene was amplified using the primers ggaattccatatggctattccaaaattaca (forward) and ccccctcgagtcattatttcacctcgcgggagag (reverse). Using the underlined *Nde*1 and *Xho*I sites, *entB* was cloned into a Novagen pET15b vector for expression. The *menF* gene was similarly amplified from a whole cell template using the primers ggaattccatatgcaatcacttactacggcgct (forward) and cccaagcttgatatgaatcggtaatgatgcgac (reverse). The *menF* gene was then cloned into the *Nde*1 and *Hin*dIII sites of a Novagen pET28b vector. Both MenF and EntB were expressed as previously reported for *E. coli* MenF (*18*). Selenomethionine (Se-Met)-substituted MenF was grown in BL21(DE3) cells in minimal media. After 8 h of growth at 37 °C, endogenous methionine production was down regulated by negative feedback inhibition through the addition of 100 mg/L Phe and Thr, and 50 mg/L Ile, Leu, and Val. Subsequently, 60 mg/L of Se-Met was added (*19*) and protein expression was induced overnight with 0.4 mM IPTG. Purification of all proteins was carried out using Novagen Ni-NTA metal affinity chromatography according to the manufacturer's instructions. 10 mM β-mercaptoethanol (BME) was included in all the purification steps for MenF. After metal affinity chromatography, WT, mutant, and Se-Met MenF were exchanged into 50 mM Tris, 1 mM EGTA, 5 mM BME pH 7.5 using Sephadex G-25 chromatography and concentrated to 25 mg/mL using a Millipore YM-30 centriplus. Aliquots (60 μL) of MenF were frozen in liquid N_2 and stored at −80 °C. After metal affinity chromatography EntB was exchanged into 25 mM Tris-HCl, 5 mM DTT, pH 8.0 and concentrated to 400 μM. Glycerol was added to 50% and EntB was stored at −20 °C. MenF protein concentration was determined using an extinction coefficient of 71305 M^{-1} cm^{-1} at 280 nm calculated using the EXPASY protparam tool (http://us.expasy.org/tools/protparam.html). Protein concentrations calculated using this extinction coefficient correlated well with determinations made using the Bradford assay. The MenF mutants Lys190Ala, Glu240Gln, Leu255Ala, Ala344Thr, and Arg387Ala were prepared using QuikChange mutagenesis (Stratagene, La Jolla, CA) and purified as described above for the WT enzyme.

CD Spectra. The far-UV CD spectra of the wild-type MenF protein and its mutant variants were recorded at a protein concentration of 20 μM in 50 mM Tris buffer pH 7.5 at 37 °C by using an AVIV 62 DS spectrometer equipped with a Peltier temperature control unit.

Enzyme Kinetics. MenF was assayed in a coupled reaction using the isochorismatase EntB, which converts isochorismate to 2,3-dihydro-2,3-dihydroxybenzoate (*20*). All coupled reactions were performed in 200 mM Tris pH 7.5, 1 mM EGTA, 1 mM DTT. After ensuring that the EntB reaction was not limiting, kinetic parameters were obtained by varying the concentrations of both $MgCl_2$ and chorismate. Activity was monitored on a Varian CARY 100 spectrophotometer at 37 °C by following the increase in absorbance at 275 nm using an extinction coefficient of 5520 cm^{-1} M^{-1} (*20*). The method described by Mildvan and co-workers (*21*) was used to obtain the kinetic parameters shown in Scheme 1, which is based on the general rate equation (eq 1) for a ternary complex random order mechanism.

Scheme 1: Kinetic Scheme for the MenF Reaction

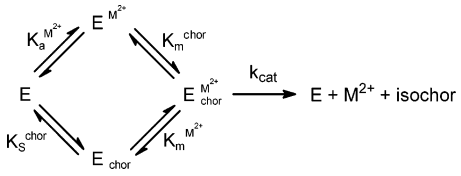

$$v = (V_{max}[Mg^{2+}][S])/(\beta K_a^{Mg2+} K_S^{chor} + \beta K_a^{Mg2+}[S] + \beta K_S^{chor}[Mg^{2+}] + [Mg^{2+}][S]) \quad (1)$$

To determine the affinity of the enzyme for Mg^{2+} in the absence (K_a^{Mg2+}) and presence (K_m^{Mg2+}) of chorismate, initial velocities were measured while varying the [chorismate] at several fixed [Mg^{2+}]. A double reciprocal plot ($1/v$ against 1/[chorismate]) of these data gave a family of curves with slopes and intercepts as a function of [Mg^{2+}]. Subsequent plots of the slopes against 1/[Mg^{2+}] and intercepts against 1/[Mg^{2+}] yielded K_a^{Mg2+} and K_m^{Mg2+}, respectively, while the latter plot also furnished k_{cat}. An analogous procedure was used to determine the affinity of the enzyme for chorismate in the absence (K_S^{chor}) and presence (K_m^{chor}) of Mg^{2+}. Note that in eq 1, $\beta K_S^{chor} = K_m^{chor}$ while $\beta K_a^{Mg2+} = K_m^{Mg2+}$.

Crystallization. WT MenF (25 mg/mL) was crystallized by vapor diffusion. 1 μL of MenF was mixed with 1 μL of a reservoir solution containing 0.1 M Hepes pH 7.5, 0.8 M potassium sodium tartrate tetrahydrate and equilibrated against the same reservoir solution. Se-Met-MenF (25 mg/mL) was crystallized by mixing 1 μL of protein with 1 μL of a reservoir solution containing 0.05 M KH_2PO_4 and 10−20% w/v PEG8000.

Data Collection and Structure Determination. Diffraction data were collected at beamline X26-C at the National Synchrotron Light Source, Brookhaven National Laboratory. For Se-Met labeled crystals, the wavelengths were chosen on the basis of the fluorescence spectrum taken at the beamline. Data were collected for two wavelengths corresponding to a high energy remote wavelength (0.9745 Å) and the inflection point (0.97971 Å). WT and Se-Met crystals diffracted to 2.5 Å and 3.0 Å, respectively. All data sets were processed, scaled, and integrated using HKL2000 (*22*). Both the WT and Se-Met crystals belonged to the tetragonal space group $P4_32_12$ with $a = b = 146.41$ Å and $c = 125.60$ Å and contained 2 molecules in the asymmetric unit. Se-Met data were used for initial phase determination using SOLVE (*23*). SOLVE located ten out of fourteen selenium positions in the asymmetric unit, which were used for initial phasing. Phases were further improved by density modification using RESOLVE (*24*), and a clear interpretable electron density map was obtained, which was extended to the full resolution

Table 1: MenF Data Collection and Refinement Statistics[a]

	Se-inflection	Se-remote	native
Data Collection			
wavelength (Å)	0.9800	0.9795	1.2536
resolution (Å)	3.0	3.0	2.5
no. of reflections (measd)	229837	301765	433357
no. of reflections (unique)	28063	28112	47352
completeness (%)	99.9	99.9	99.1
R_{merge} (%)	7.6 (32.7)	8.1 (37.0)	9.1 (41.2)
$\langle I\rangle/\langle\sigma I\rangle$	17.7 (4.6)	19.8 (5.2)	39.4 (2.4)
no. of sites	11		
mean figure of merit 4.0 Å	0.57		
Refinement			
resolution range (Å)			30−2.5
reflections			44680
R_{cryst}			0.229
R_{free}			0.276
no. of atoms			
protein			6695
ligands			20
water			150
rms deviation			
in bond length (Å)			0.015
in angles (deg)			1.59
Ramachandran statistics (%)			88.4/9.6/0.7/1.3

[a] $R_{merge} = \sum_{hkl}\sum_i|I_i - \langle I\rangle|/\sum_{hkl}\sum_i I$ where I_i is the ith measurement and $\langle I\rangle$ is the weighted mean of all measurements of I. $\langle I\rangle/\langle\sigma I\rangle$ indicates the average of the intensity divided by its average standard deviation. Numbers in parentheses refer to the respective highest resolution data shell in each data set. $R_{cryst} = \sum||F_o| - |F_c||/\sum|F_o|$ where F_o and F_c are the observed and calculated structure factor amplitudes. R_{free} same as R_{cryst} for 5% of the data randomly omitted from the refinement. Ramachandran statistics indicate the fraction of residues in the most favored, additionally allowed, generously allowed, and disallowed regions of the Ramachandran diagram, as defined by the program PROCHECK (*28*).

using DM (*25*, *26*). The model was built manually with O. Several cycles of rigid body refinement with REFMAC (*27*) reduced the R_{free} to 0.43. After a few cycles of model building and restrained refinement, the R_{free} was 0.305 for the resolution range 25−2.5 Å. At this stage of refinement water molecules were added, and after few cycles of further refinement the stereochemistry of the model was checked with PROCHECK (*28*). Data and refinement statistics are shown in Table 1.

RESULTS

Protein Purification. MenF was purified in yields of up to 70 mg/L using Ni-NTA metal affinity chromatography. As previously reported (*18*), MenF rapidly lost activity at 4 °C and was therefore stored at −80 °C at a concentration of 25 mg/mL. In addition to being kinetically compromised by overnight storage at 4 °C, MenF lost its ability to crystallize. In contrast, EntB, which was similarly purified using Ni-NTA chromatography, was stable for >1 year in 50% glycerol at −20 °C (*29*).

Sequence Alignment. Using the Blast alignment tool, MenF is 28% identical and 43% similar (C-terminal 254 residues) to the TrpE subunit of anthranilate synthase from *S. marcescens* (AS-sm). The AS-sm structure with bound Mg^{2+}, pyruvate, and benzoate has been reported (*12*). Eighteen of the 26 amino acids within 6 Å of the bound ligands are conserved in MenF. Of the 8 residues that differ between the two enzymes, none of the side chains directly contact the ligand and only Lys190, Leu255, and Ala344 are unique to ICS enzymes. Based on a sequence alignment (*30*) of more than 1000 MST sequences, Lys190 is conserved in all enzymes which hydroxylate chorismate but is primarily Gln in enzymes which aminate chorismate. The position corresponding to MenF Leu255 is generally conserved as a large hydrophobic residue and is part of larger variable motif. The position corresponding to MenF Ala344 is conserved in all ICS enzymes but is replaced by a Thr in salicylate synthases and AS enzymes, and Ser in PabB. MenF Ala344 was mutated to a Thr in an attempt to convert MenF into a salicylate synthase; however, the Ala344Thr MenF enzyme was inactive. A sequence alignment including the active site residues of all characterized MST enzymes is shown in Figure 4. The entire amino acid sequences are not shown but instead just those sequences containing residues homologous to the 26 residues within 6 Å of the bound Mg^{2+}, benzoate, and pyruvate in the AS-sm structure.

Kinetic Analysis of WT and Mutant MenF Enzymes. MenF was characterized using a previously described coupled assay for *E. coli* EntC that utilized the isochorismatase EntB (*29*). Data were analyzed using the method described by Mildvan and co-workers (*21*) to extract the kinetic parameters shown in Scheme 1. WT MenF had a k_{cat} value of 213 ± 5 min^{-1} and K_m values of 192 ± 7 and 770 ±12 μM for chorismate (K_m^{chor}) and Mg^{2+} (K_m^{Mg2+}), respectively, similar to previously published values (*18*, *31*). The K_m^{Mg2+} value is 4-fold lower than the kinetically determined affinity of Mg^{2+} for the free enzyme (K_a^{Mg2+}), indicating that Mg^{2+} binds more tightly to the enzyme in the presence of chorismate. A smaller effect on chorismate binding in the absence (K_s^{chor}) and presence (K_m^{chor}) of Mg^{2+} was observed. No activity could be detected for any of the point mutants (Lys190Ala, Glu240Gln, Ala344Thr, and Arg387Ala) with the exception of Leu255Ala, for which the k_{cat} value was decreased by an order of magnitude compared to the WT enzyme. CD spectra were obtained for all the mutant enzymes, and the resulting spectra were identical to that of the wild-type enzyme (Figure 5), suggesting that mutagenesis had not altered the overall structure of the protein. The four equilibrium constants of MenF Leu255Ala all had similar values compared to the WT enzyme, with the largest effect on K_m^{Mg2+}, which was increased 3-fold. The results are presented in Table 2.

Structure of MenF. The two molecules in the asymmetric unit of the apo MenF structure have the α/β fold first characterized by Knöchel et al. in the structure of AS from *S. solfataricus* (*32*). Continuous electron density was seen for both molecules for residues 2−429 out of 431 possible residues which can be superimposed with a rms deviation of 0.42 Å for all Cα atoms. MenF shares high structural similarity to the TrpE subunits of anthranilate synthase (AS) from *Sulfolobus solfataricus* (AS-ss) (*32*), *Salmonella typhimurium* (AS-st) (*33*), and *Serratia marcescens* (*12*) as well as the salicylate synthase Irp9 (*34*) and PabB, the aminodeoxychorismate synthase from *E. coli* (*16*).

Many AS enzymes are feedback inhibited by Trp, and the regulatory binding site has been identified in both the AS-sm (*12*) and AS-st (*33*) structures complexed with tryptophan. The presence of an exogenous Trp essential for structural integrity in PabB suggested that other MST enzymes, including MenF, bind Trp in a similar manner (*16*). However, the addition of Trp has no effect on MenF activity, and the MenF structure does not contain an analogous Trp binding

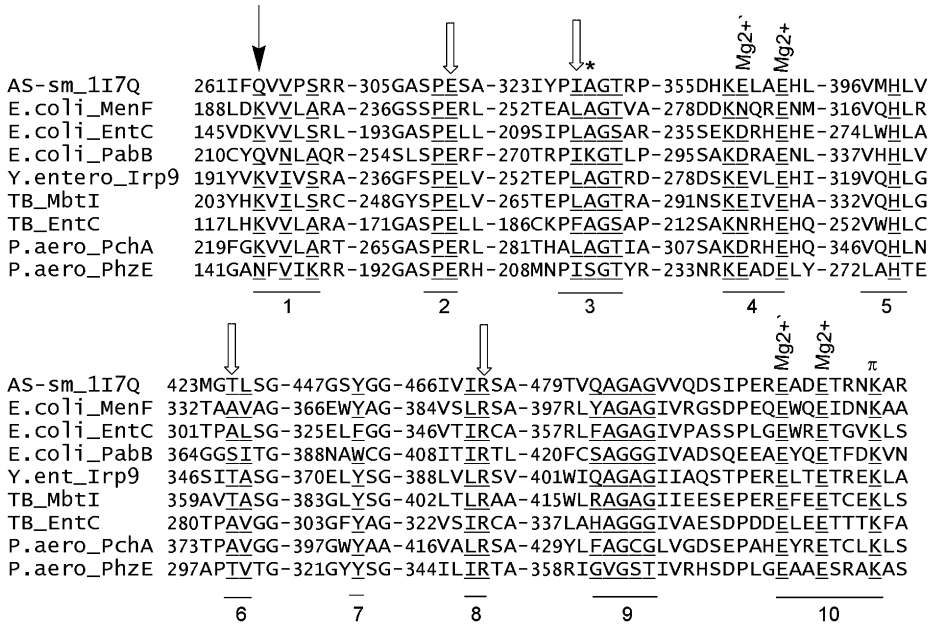

FIGURE 4: Active site sequence conservation in the MST family. The alignment explores sequence conservation in the MST family at the 26 positions within 6 Å of the Mg^{2+}, benzoate, and pyruvate in the AS-sm structure (*12*). The underlined residues can be assigned to the 10 labeled motifs which collectively signify a MST enzyme. Arrows indicate the location of site directed mutants of MenF. The asterisk indicates the position of the Lys essential for PabB activity. The solid arrow indicates the position homologous to the water activating base in MenF, Lys190. "Mg^{2+}" and "$Mg^{2+'}$" designate the conserved residues which directly and via water, respectively, coordinate Mg^{2+}. "π" indicates the position of an absolutely conserved Lys.

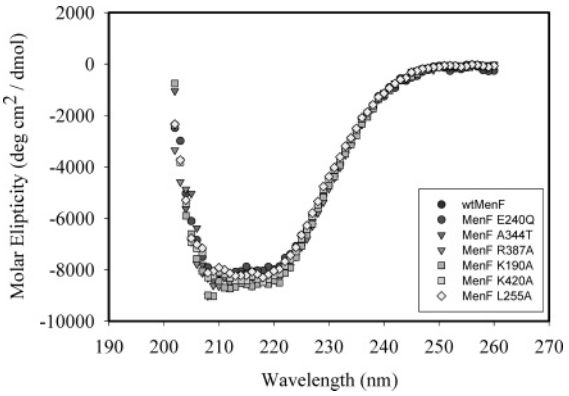

FIGURE 5: CD spectra of wild-type and mutant MenF proteins.

Table 2: Kinetic Evaluation of Wild-Type and Mutant[a] MenF Enzymes

enzyme[b]	k_{cat} (min^{-1})	K_a^{Mg2+} (μM)	K_a^{Mg2+} (μM)	K_s^{chor} (μM)	K_m^{chor} (μM)
wild-type	213 ± 5	3000 ± 500	770 ± 12	320 ± 5	192 ± 7
Leu255Ala	19 ± 1	4700 ± 550	2100 ± 95	433 ± 22	319 ± 13

[a] K_a^{Mg2+} and K_m^{Mg2+} are the dissociation constants of Mg^{2+} for the free enzyme and enzyme−chorismate complex, respectively. K_s^{chor} and K_m^{chor} are the dissociation constants of chorismate for the free enzyme and the enzyme−Mg^{2+} complex, respectively. [b] The Lys190, Glu240Gln, Ala344Thr, and Arg387Ala MenF mutants had no detectable activity.

site. Instead, the side chain of Trp55 partially occupies the position of the external Trp side chain in the Trp inhibited protein structures. A comparison with other MST enzymes reveals that the loop connecting β-strands β2 and β3 (residues Q57−D61), which contains the Trp binding residues in AS and PabB, is shortened in MenF and is disordered in the unliganded AS-ss enzyme (*32*) (PDB ID 1QDL). This comparison also reveals that a β-hairpin, which extends from the β-sheet of the second domain and is present in PabB (PDB ID 1K0E), AS-sm (PDB ID 1I7Q, 1I7S), and AS-st (PDB ID 1I1Q), is absent in MenF.

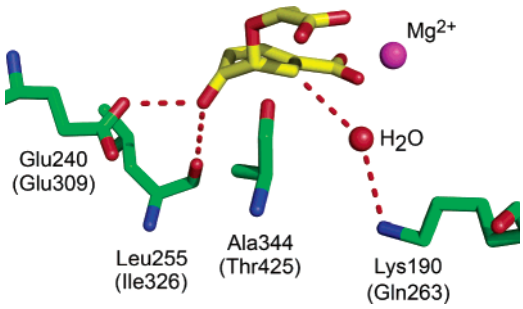

FIGURE 6: Conserved MenF active site residues with superimposed chorismate ligand. MenF was superimposed on the AS-sm structure and chorismate was superimposed onto the ring of the bound AS-sm benzoate ligand. The chorismate is in a diaxial conformation. An ordered water molecule (H_2O) from the homologous Irp9 structure (PDB ID 2FN1) is also included. MenF residues are labeled, and the corresponding AS-sm residues are given in parentheses. The side chain of Glu240 and the backbone carbonyl of Leu255 are positioned to interact with the C4 hydroxyl of chorismate. The backbone carbonyl of Ala344 is adjacent to both the C2 and C3 chorismate carbons. Lys190 is invariant and is positioned to activate the ordered water molecule for attack at the C2 carbon of chorismate. The figure was created using pymol (*40*).

DISCUSSION

Glu240, Leu255, and Ala344: Isomerization. When the MenF structure is superimposed on AS-sm, the only residues adjacent to the face of the AS-sm ligand where isomerization is proposed to occur are MenF Glu240, Ala344, and Leu255 (Figure 6). The corresponding residues in the AS-sm structure are Glu309, Thr425, and Ile326. Leu255 is conserved as a large hydrophobic residue while Ala344 is conserved in isochorismate synthases but is replaced by a Thr in anthra-

nilate and salicylate synthases. Although this might suggest that the presence of Ala or Thr at position 334 controls the retention or elimination of pyruvate in this enzyme family, replacement of Ala344 in MenF with a Thr residue resulted in an inactive enzyme. In addition, we note that a Thr is observed at this position in aminodeoxyisochorismate synthase PhzE (*35*) (Figure 4), which catalyzes aminodeoxychorismate formation without cleavage of the pyruvate side chain. As shown in Figure 6, if chorismate is modeled onto the benzoate ring of the AS-sm structure and MenF is superimposed, the backbone carbonyl oxygen of Ala344 (Thr425 As-sm) is directed toward the C3 carbon of chorismate. The homologous carbonyl group has also been proposed to interact with the C2 substituent of isochorismate in the salicylate synthase Irp9 and aminodeoxychorismate in anthranilate synthase (*36*, *37*). The side chain of AS-sm Thr425 forms a hydrogen bond with the side chain of a conserved glutamate, Glu309, a residue that is thought to assist in the elimination of the chorismate C4 hydroxyl group. In agreement with the proposed importance of this glutamate, replacement of the homologue in MenF (Glu240) with a Gln results in an inactive enzyme. Like the side chain of Glu240, the backbone carbonyls of MenF Leu255 and AS-sm Ile326 are also positioned to interact with the C4 hydroxyl of chorismate. When MenF Leu255 was mutated to Ala, k_{cat}/K_M for chorismate and Mg^{2+} decreased significantly by 21 and 46-fold, respectively. Thus, even subtle changes in active site architecture impact catalysis. The effect of the Leu255Ala substitution on substrate isomerization could result from an alteration in the interaction between the backbone carbonyl of this residue and the substrate and/or repositioning of the substrate in the active site such that stabilization of the rate-limiting transition state is compromised.

Allosteric Regulation. In an average bacterial cell there can be six or more enzymes competing for chorismate (Figure 1). The interaction of substrate with these enzymes is regulated by both allosteric and genetic mechanisms. AS-sm is feedback inhibited by Trp (*12*). In AS-sm, binding of Trp to a site that is distinct from the active site causes several conformational changes including a rotation of Glu309 by more than 90°, so that it can no longer interact with the C4 hydroxyl of chorismate. In our MenF structure, the homologous residue (Glu240) aligns well with Glu309 in the benzoate bound AS-sm structure. Analysis of the region in MenF where the As-sm Trp binding site is located reveals that this site is occupied by the side chain of Trp55. In agreement with this observation and in contrast to all characterized enzymes which aminate chorismate, MenF is not kinetically or structurally affected by Trp. Instead, MenF is thought to be regulated at the transcriptional level based on the identification of a putative cAMP dependent regulatory site upstream of the start codon (*31*).

Lys190: The Active Site Base. The original proposed transition state for isomerization in the MST family is shown in Figure 2A (*10*, *11*). This model was based on the requirement for Mg^{2+}, as well as on inhibition data obtained using a series of high affinity inhibitors that preferentially mimic a pseudoaxial transition state with Mg^{2+} coordinated to both the incoming nucleophile and the departing C4 chorismate hydroxyl group. However, the crystal structures of Irp9 and AS-sm show that Mg^{2+} binds in an alternative conformation, coordinated by the C1 chorismate carboxylate

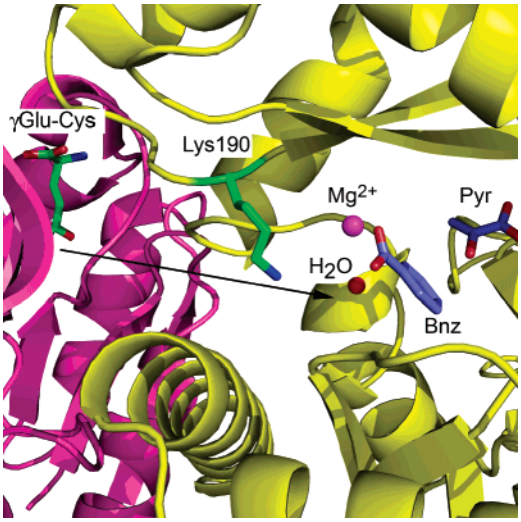

FIGURE 7: Lys190 activates water for attack at the C2 of chorismate. MenF (yellow) was overlaid on the TrpE subunit of 1I7Q AS-sm. The 1I7Q structure includes both TrpG (glutamine amidotransferase, shown in magenta) and TrpE (not shown) subunits. TrpG provides ammonia for incorporation into anthranilate by TrpE. By analogy, MenF incorporates a hydroxyl group from solvent water into chorismate and the incoming nucleophiles in both reactions are proposed to enter their respective active sites in an identical manner. When the structures are overlaid, MenF Lys190 is in a direct line between the TrpG and MST active sites, shown by an arrow, and is positioned to activate water for attack at the C2 of chorismate. No other side chains are available to aid in nucleophile transfer. The figure was created using pymol (*40*).

and a series of universally conserved acidic residues (*12*). Although binding of a second Mg^{2+} is plausible, there are no side chains available to coordinate the metal in order that it could interact with the attacking and departing groups. Instead, we hypothesize that Lys190 in MenF and the corresponding residue in all MST enzymes, specifically Lys193 in Irp9 and Gln263 in AS-sm, is responsible for directing and activating the exogenous nucleophile. This hypothesis is supported by the observation that the Lys190Ala mutant is inactive. Superposition of MenF with AS-sm reveals that Lys190 is positioned at the junction between the TrpE and TrpG subunits of AS-sm (Figure 7). Anthranilate synthase is a $TrpE_2TrpG_2$ heterotetramer in which TrpG provides ammonia from glutamine, which is used by TrpE to form anthranilate. In AS-sm there is a 23 Å channel between the active sites of TrpG and TrpE along which the ammonia is thought to diffuse. TrpG generates ammonia from Gln and forms a covalent glutamyl thioester (Figure 7). Although MenF lacks an additional subunit corresponding to TrpG, it is likely that the incoming solvent nucleophile enters the active site in an identical manner, and Liu et al. have previously established that the incoming nucleophile in ICS is solvent derived (*20*). Lys190 is the only residue along this channel that can activate the nucleophile. The corresponding residue in related enzymes catalyzing chorismate amination (TrpE, PabB, ADIC synthase (PhzE)) is primarily Gln, but Asn and Glu are also observed.

Although the solution p*K* of lysine is approximately 10.8, the MenF protein environment must modulate the Lys190 ϵ-amino group such that it can act as an efficient base at physiological pH. Our structure reveals that Lys190 is shielded from solvent and faces into the protein where its side chain may form hydrophobic interactions with Val193

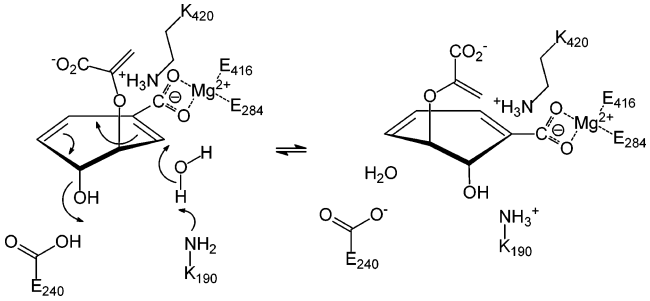

FIGURE 8: Proposed MenF mechanism. The C1 carboxylate of chorismate is bound to a Mg^{2+} ion which is also coordinated by Glu284 and Glu416. Lys190 is the base that assists in the attack of water at the C2 carbon of chorismate. This results in an S_N2'' reaction with a rearrangement of the 1−2, 5−6 double bonds and elimination of the C4 hydroxyl. Glu240 is essential for activity and is in a position to provide acid catalysis for the elimination of the C4 hydroxyl group. This mechanism can be extended to all members of the MST enzyme family with primarily Gln replacing Lys190 in chorismate aminating enzymes.

and Val405. The ϵ-amino group hydrogen bonds with either the side chain or backbone of Glu284. These interactions are conserved throughout the family and in the salicylate-bound structure of the salicylate synthase Irp9, the corresponding Lys193 interacts with Ile195 and Ile409 and the ϵ-amino hydrogen bonds to the backbone carbonyl of Glu284. In a recent study on the enzyme Ubc9, Yunus and Lima (*38*) concluded that desolvation was the primary driving force for the 2.8 pH unit reduction in p*K* of Lys524. The unique microenvironment within the MenF protein adjacent to the active site may provide an analogous environment and promote deprotonation of Lys190, allowing it to act as the catalytic base.

He et al. have proposed a general mechanism for the MST family in which catalysis is initiated by the attack of a main chain or exogenous nucleophile at the C2 carbon of chorismate (*14*). The identification of MenF Lys190 as the base responsible for activating the water nucleophile in MenF supports and extends this mechanism. Based on the available data, our proposed mechanism for the MenF reaction is shown in Figure 8. Our model is further supported by the recently reported structure of Irp9 with bound Mg^{2+}, pyruvate, and salicylate. In the Irp9 salicylate-bound structure, there is an ordered water molecule located in the channel described above that is 3.8 Å from the C2 carbon of the bound salicylate and 2.8 Å from the ϵ-amino of Lys193, the residue in Irp9 that is homologous to MenF Lys190.

The MST Superfamily. More than 1000 amino acid sequences having homology to *E. coli* MenF can be identified in the National Center for Biotechnology (NCBI) genomic data base (*39*). This unique family catalyzes at least five distinct transformations of chorismate using a conserved structural template. The homology among family members suggests that identifiable differences in active site residues may be sufficient to explain the various enzyme activities that are observed. In the present work we show that MST enzymes that either hydroxylate or aminate chorismate can be distinguished based on the identity of the residue at the position occupied by Lys190 in MenF. This residue is a Lys in all enzymes which hydroxylate chorismate and primarily conserved as Gln in enzymes which aminate chorismate.

SUMMARY

Structural and kinetic data on MenF, the menaquinone-specific isochorismate synthase from *E. coli*, identify specific residues involved in the more general mechanism proposed by He et al. (*14*) for the MST enzyme family. We propose that Lys190 in MenF activates water for attack at the C2 of chorismate and that residues homologous to Lys190 perform a corresponding role in other members of the MST enzyme family. Since the MST enzymes catalyze the initial step in biosynthetic pathways that are essential for many organisms, they represent a wealth of potential novel drug targets. Along these lines, compounds that inhibit two or more members of the MST family simultaneously would be particularly useful. This in turn will require a detailed understanding of the mechanistic features that distinguish between the MST enzymes, all of which bind chorismate but perform catalytically distinct transformations. An important milestone in these studies will be to use our knowledge to rationally interchange activities within the MST family. Remaining questions include the order of bond formation and cleavage and the exact geometry at the active site that allows catalysis to proceed. Ongoing crystallographic and isotopic labeling studies will address these questions.

ACKNOWLEDGMENT

We thank Dr. Peter Kast of the ETH for providing *E. coli* strain KA12, which was used as a source of chorismate. Atomic coordinates have been deposited in the Protein Data Bank with access code 2EUA.

REFERENCES

1. Dosselaere, F., and Vanderleyden, J. (2001) A metabolic node in action: chorismate-utilizing enzymes in microorganisms, *Crit. Rev. Microbiol. 27*, 75−131.
2. Olson, R. E. (1984) The function and metabolism of vitamin K, *Annu. Rev. Nutr. 4*, 281−337.
3. Truglio, J. J., Theis, K., Feng, Y., Gajda, R., Machutta, C., Tonge, P. J., and Kisker, C. (2003) Crystal structure of *Mycobacterium tuberculosis* MenB, a key enzyme in vitamin K2 biosynthesis, *J. Biol. Chem. 278*, 42352−42360.
4. Collins, M. D., Goodfellow, M., Minnikin, D. E., and Alderson, G. (1985) Menaquinone composition of mycolic acid-containing actinomycetes and some sporoactinomycetes, *J. Appl. Bacteriol. 58*, 77−86.
5. Gomez, J. E., and McKinney, J. D. (2004) M. tuberculosis persistence, latency, and drug tolerance, *Tuberculosis 84*, 29−44.
6. Weinstein, E. A., Yano, T., Li, L., Avarbock, D., Helm, D., McColm, A. A., Duncan, K., Lonsdale, J. T., and Rubin, H. (2005) Inhibitors of type II NADH:menaquinone oxidoreductase represent a class of antitubercular drugs, *Proc. Natl. Acad. Sci. U.S.A. 102*, 4548−4553.
7. Cole, S. T., Brosch, R., Parkhill, J., Garnier, T., Churcher, C., Harris, D., Gordon, S. V., Eiglmeier, K., Gas, S., Barry, C. E. r., Tekaia, F., Badcock, K., Basham, D., Brown, D., Chillingworth, T., Connor, R., Davies, R., Devlin, K., Feltwell, T., Gentles, S., Hamlin, N., Holroyd, S., Hornsby, T., Jagels, K., and Barrell, B. G. (1998) Deciphering the biology of *Mycobacterium tuberculosis* from the complete genome sequence, *Nature 393*, 537−544.
8. Sasso, S., Ramakrishnan, C., Gamper, M., Hilvert, D., and Kast, P. (2005) Characterization of the secreted chorismate mutase from the pathogen *Mycobacterium tuberculosis*, *FEBS J. 272*, 375−389.
9. Gallagher, D. T., Mayhew, M., Holden, M. J., Howard, A., Kim, K. J., and Vilker, V. L. (2001) The crystal of chorismate lyase shows a new fold and a tightly retained product, *Proteins 44*, 304−311.
10. Kozlowski, M. C., Tom, N. J., Seto, C. T., Sefler, A. M., and Bartlett, P. A. (1995) Chorismate-utilizing enzymes isochorismate

synthase, anthranilate synthase, and P-aminobenzoate synthase-mechanistic insight through inhibitor design, *J. Am. Chem. Soc. 117*, 2128−2140.
11. Walsh, C. T., Liu, J., Rusnak, F., and Sakaitani, M. (1990) Molecular studies on enzymes in chroismate metabolism and the enterobactin biosynthetic pathway, *Chem. Rev. 90*, 1105−1129.
12. Spraggon, G., Kim, C., Nguyen-Huu, X., Yee, M. C., Yanofsky, C., and Mills, S. E. (2001) The structures of anthranilate synthase of Serratia marcescens crystallized in the presence of (i) its substrates, chroismate and glutamine, and a product, glutamate, and (ii) its end-product inhibitor, L-tryptophan, *Proc. Natl. Acad. Sci. U.S.A. 98*, 6021−6026.
13. Kerbarh, O., Ciulli, A., Howard, N. I., and Abell, C. (2005) Salicylate biosynthesis: overexpression, purification, and characterization of Irp9, a bifunctional salicylate synthase from *Yersinia enterocolitica*, *J. Bacteriol. 187*, 5061−5066.
14. He, Z., Stigers Lavoie, K. D., Bartlett, P. A., and Toney, M. D. (2004) Conservation of mechanism in three chorismate-utilizing enzymes, *J. Am. Chem. Soc. 126*, 2378−2385.
15. Bulloch, E. M., Jones, M. A., Parker, E. J., Osborne, A. P., Stephens, E., Davies, G. M., Coggins, J. R., and Abell, C. (2004) Identification of 4-amino-4-deoxychorismate synthase as the molecular target for the antimicrobial action of (6s)-fluoroshikimate, *J. Am. Chem. Soc. 126*, 9912−9913.
16. Parsons, J. F., Jensen, P. Y., Pachikara, A. S., Howard, A. J., Eisenstein, E., and Ladner, J. E. (2002) Structure of *Escherichia coli* aminodeoxychorismate synthase: architectural conservation and diversity in chorismate-utilizing enzymes, *Biochemistry 41*, 2198−2208.
17. Grisostomi, C., Kast, P., Pulido, R., Huynh, J., and Hilvert, D. (1997) Efficient in vivo synthesis and rapid purification of chorismic acid using an engineered *Escherichia coli* strain, *Bioorg. Chem. 25*, 297−305.
18. Daruwala, R., Bhattacharyya, D. K., Kwon, O., and Meganathan, R. (1997) Menaquinone (vitamin K2) biosynthesis: overexpression, purification, and characterization of a new isochorismate synthase from *Escherichia coli*, *J. Bacteriol. 179*, 3133−3138.
19. Doublie, S. (1997) Preparation of selenomethionine substituted proteins for phase determination, *Methods Enzymol. 276*, 523−530.
20. Liu, J., Quinn, N., Berchtold, G. A., and Walsh, C. T. (1990) Overexpression, purification, and characterization of isochorismate synthase (EntC), the first enzyme involved in the biosynthesis of enterobactin from chorismate, *Biochemistry 29*, 1417−1425.
21. Legler, P. M., Lee, H. C., Peisach, J., and Mildvan, A. S. (2002) Kinetic and magnetic resonance studies of the role of metal ions in the mechanism of escherichia coli GDP-mannose mannosyl hydrolase, an unusual nudix enzyme, *Biochemistry 41*, 4655−4668.
22. Otwinowski, Z., and Minor, W. (1997) Processing of X-ray diffraction data collected in oscillation mode, *Methods Enzymol. 276*, 307−326.
23. Terwilliger, T. C., and Berendzen, J. (1999) Automated MAD and MIR structure solution, *Acta Crystallogr. D55*, 849−861.
24. Terwilliger, T. C. (2000) Maximum-likelihood density modification, *Acta Crystallogr. D56*, 965−972.
25. Cowtan, K. (1994) An automated procedure for phase improvement by density modification, *Joint CCP4 and ESF-EACBM Newsletter on Protein Crystallography 31*, 34−38.
26. Bailey, S. (1994) The Ccp4 Suite-programs for protein crystallography, *Acta Crystallogr. D50*, 760−763.
27. Murshudov, G. N., Vagin, A. A., and Dodson, E. J. (1997) Refinement of macromolecular structures by the maximum-likelihood method, *Acta Crystallogr. D53*, 240−255.
28. Laskowski, R. A., MacArthur, M. W., Moss, D. S., and Thornton, J. M. (1993) The lattice constant of a nonperfect crystal measured by X-ray diffraction, *J. Appl. Crystallogr. 26*, 280−283.
29. Rusnak, F., Liu, J., Quinn, N., Berchtold, G. A., and Walsh, C. T. (1990) Subcloning of the enterobactin biosynthetic gene entB: expression, purification, characterization and substrate specificity of isochorismatase, *Biochemistry 29*, 1425−1435.
30. Altschul, S. F., Gish, W., Miller, W., Myers, E. W., and Lipman, D. J. (1990) Basic local alignment search tool, *J. Mol. Biol. 215*, 403−410.
31. Dahm, C., Muller, R., Schulte, G., Schidt, K., and Leistner, E. (1998) The role of isochorismate hydroxymutase genes entC and menF in enterobactin and menaquinone biosynthesis in Escherichia coli, *Biochim. Biophys. Acta 1425*, 377−386.
32. Knochel, T., Ivens, A., Hester, G., Gonzalez, A., Bauerle, R., Wilmanns, M., Kirschner, K., and Jansonius, J. N. (1999) The crystal structure of anthranilate synthase from Sulfolobus solfataricus: functional implications, *Proc. Natl. Acad. Sci. U.S.A. 17*, 9479−9484.
33. Morollo, A. A., and Eck, M. J. (2001) Structure of the cooperative allosteric anthranilate synthase from Salmonella typhimurium, *Nat. Struct. Biol. 8*, 243−247.
34. Kerbarh, O., Chirgadze, D. Y., Blundell, T. L., and Abell, C. (2006) Crystal structures of *Yersinia enterocolitica* salicylate synthase and its complex with the reaction products salicylate and pyruvate, *J. Mol. Biol. 357*, 524−534.
35. Mavrodi, D. V., Ksenzenko, V. N., Bonsall, R. F., Cook, R. J., Boronin, A. M., and Thomashow, L. S. (1998) A seven-gene locus for synthesis of phenazine-1-carboxylic acid by Pseudomonas fluorescens 2-79, *J. Bacteriol. 180*, 2541−2548.
36. Payne, R. J., Kerbarh, O., Miguel, R. N., Abell, A. D., and Abell, C. (2005) Inhibition studies on salicylate synthase, *Org. Biomol. Chem. 3*, 1825−1827.
37. Payne, R. J., Toscano, M. D., Bulloch, E. M., Abell, A. D., and Abell, C. (2005) Design and synthesis of aromatic inhibitors of anthranilate synthase, *Org. Biomol. Chem. 3*, 2271−2281.
38. Yunus, A. A., and Lima, C. D. (2006) Lysine activation and functional analysis of E2-mediated conjugation in the SUMO pathway, *Nat. Struct. Mol. Biol. 13*, 491−499.
39. Pruitt, K. D., Tatusova, T., Maglott, D. R. (2005) NCBI Reference Sequence (RefSeq): a curated non-redundant sequence database of genomes, transcripts and proteins, Nucleic Acids Res. 33, D501−D504.
40. DeLano, W. L. (2002) The PyMOL Molecular Graphics System on World Wide Web *http://www.pymol.org.*

BI0608515